TASK QUARTERLY 12 No 3, 147–158

DEVELOPMENT OF VORTEX STRUCTURES IN A TURBINE STAGE ROTOR PASSAGE

JERZY ŚWIRYDCZUK

Institute of Fluid-Flow Machinery, PAS,
Fiszera 14, 80-952 Gdansk, Poland
jsk@imp.gda.pl

(Received 30 April 2008: revised manuscript received 29 May 2008)

Abstract: The article analyses the formation and development of horseshoe vortices in a high-pressure turbine stage rotor passage. Two turbine stages are examined: a standard performance stage, revealing regular performance characteristics and distributions of flow parameters, and a low-efficiency stage in which a large separation zone is observed in rotor passages. In the latter stage the interaction of the hub horseshoe vortex with the separation structures has been found to take a highly unsteady and periodic course and be a source of remarkable flow fluctuations.

Keywords: turbine stage, vortex structures, CFD analysis

1. Introduction

The flow through a turbine stage, even treated as an isolated machine, is extremely complex due to the presence of numerous secondary flows and vortex structures in the stator and rotor cascades. Firstly, horseshoe vortices are formed at blade leading edges of the stator and rotor blades, near the hub and tip endwalls. At the same time the trailing edges of the stator and rotor blades are the sources of wakes which are shed downstream being convected with the main flow into the next cascades. The leakage flows, mixing with the main flow, frequently lead to the creation of large-scale vortices. A similar effect can be generated by flow separation, most frequently observed at the rear part of the rotor passage, near the blade trailing edge. A permanent interaction between all the abovementioned flow structures makes studying the turbine flow extremely difficult.

Computer codes developed for solving the Navier-Stokes equations are powerful and useful tools to be used for studying these flows. Theoretically, these codes, frequently refereed to as CFD (Computational Fluid Dynamics) codes, provide opportunities for taking into account all details of three-dimensional geometry of stage construction, and recording all unsteady effects of the flow structures interaction. In practice, however, economic and technical limitations make the CFD code user look for a reasonable compromise between the expected accuracy of the results to be obtained and the time necessary for performing the calculations.

The first phenomenon specific for the turbine stage as a whole, which was examined using the CFD methodology, was the stator/rotor interaction. The above name encompasses all phenomena resulting from the relative stator/rotor motion, the most remarkable of which is the unsteady interaction of stator wakes with downstream rotor blades. Each stator wake, shed from the stator blade and convected with fluid towards the rotor cascade, is cut apart by the rotor cascade. Then, when moving through the rotor passages, consecutive stator wake segments deform into pairs of opposite-rotation vortices and generate characteristic local and instantaneous flow fluctuations which, in turn, affect stage performance characteristics. An extremely high resolution of the numerical grid on which the calculations are performed is required to analyse this problem. What is worse, unlike steady-state calculations in which all important flow phenomena are assumed to take place in the boundary layer and the calculation grid is created to follow this assumption, in unsteady calculations the grid has to have a sufficiently high resolution in the entire flow area to be able to capture all the details of vortex interactions. A strategy most frequently applied in the past, especially in 3D calculations, was to perform calculations with the finest possible resolution offered by the available hardware, which left the problem of grid independence of the obtained results unsolved. An attempt to assess the minimum grid resolution for stator/rotor interaction calculations in two dimensions has been made by Arnone *et al.* [1, 2], who placed it at the level of 17 000 cells per stator or rotor passage. A similar conclusion can be formulated after comparing the experimental and numerical results obtained by Kost *et al.* [3]. Direct extrapolation of this assessment into the third dimension returns 2 000 000 cells per one passage as the minimum resolution required to secure grid independency [4].

The investigations discussed in the article concern the problem of a combined three-dimensional interaction of all vortex structures observed in a turbine stage rotor. As mentioned above, the number of structures which may take part in this interaction is rather large, and a direct approach to analyse the recorded flow distributions does not seem promising. That is why the problem has been divided into stages in which the contribution of selected individual vortices to the global flow pattern is analysed. At present, the process of formation and development of horseshoe vortices in the rotor passage is examined in various flow conditions represented by different stage performance characteristics, with a general aim to collect a variety of possible courses of vortex behaviour, applicable in unsteady vortex interaction analyses.

2. Stage geometry and flow conditions

Bearing in mind the above investigation goal it was assumed that the stages selected as the main objects of examination should generate a varying and relatively complex flow structure to provide opportunities for studying the development of horseshoe vortices in different flow conditions. At the same time the stage geometry should be representative for a relatively wide range of turbine stage constructions, to make the range of applicability of the obtained results as wide as possible. The stages were selected on the basis of steady-state results obtained on a moderate-resolution grid of an order of 400 000 cells per stator/rotor passage which is a resolution range usually used in steady-state analyses of turbine stage flows. As a result, two

stages were selected for the analysis. The first stage, referred to in the article as the reference stage, was a high-pressure turbine stage with cylindrical blades which revealed relatively good performance characteristics and regular distributions of losses, see Figure 1 – the dashed curve. At the same time the second stage of the same construction revealed significantly decreased efficiency and untypical and varying stage loss distributions, see the solid curve in Figure 1. Unlike the regular distributions in which only increased losses near the hub and tip endwalls are observed, the loss distributions recorded in the low-efficiency stage frequently revealed additional huge maxima near the rotor passage midspan sections. The entropy distribution[1] recorded in the $x0y$ section at the rotor blade trailing edge, Figure 2, suggested massive flow separation in this region, which was expected to provide an excellent opportunity to capture its possible interaction with the examined horseshoe vortices.

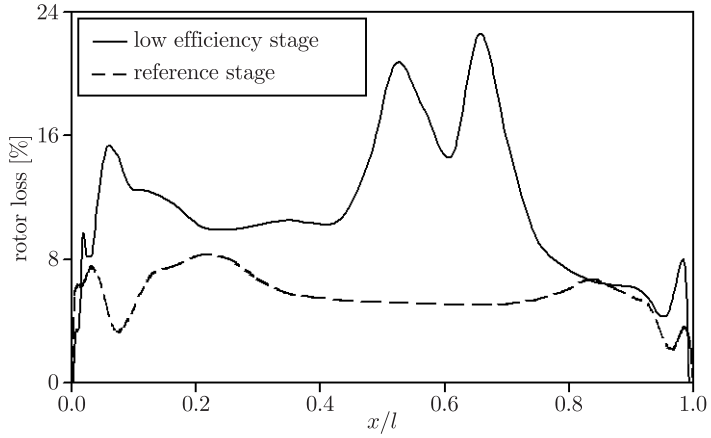

Figure 1. Spanwise distributions of rotor losses recorded at a distance $z/c = 1.78$ from the rotor blade leading edge

The general stage geometry is shown in Figure 3 which also presents a sample distribution of gridlines for a moderate-resolution grid used in the stage selection process. The problem of selecting grid parameters for further investigations in such a way that a sufficiently fine resolution for studying the development of horseshoe vortices, the object of the present analysis, could be achieved, was solved by comparing the results recorded on a series of grids with increasing resolution, starting from the grid shown in Figure 3 and ending with that of an order of 2 000 000 cells per passage. The grid selected as a result had $144 \times 120 \times 116 = 2\,004\,480$ cells in one stator passage and $144 \times 64 \times 240 = 2\,211\,840$ cells in one rotor passage. The gridline distribution revealed a comparable resolution in all three dimensions, a feature often neglected in earlier analyses presented in the literature. A fine grid resolution in the main flow area was occupied by a slightly decreased resolution in the boundary layer areas. This compromise, taking also into account the technical and economic conditions, was made with the intention to provide comparable conditions for vortex development

1. More precisely, the FlowER postprocessor produces distributions of the entropy function: $\sigma_S = p/\rho^\gamma$ rather than the entropy itself: $S = c_v \ln T + R \ln V + S_0$. This remark refers to all entropy diagrams presented in the article.

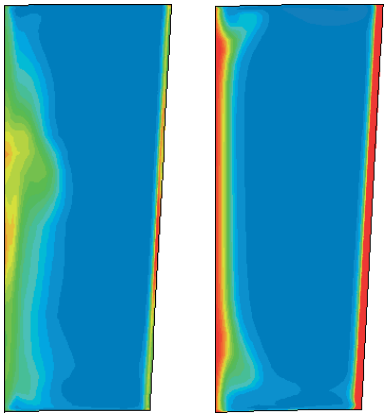

Figure 2. Entropy distributions in $x0y$ sections at rotor blade trailing edge, $z/c = 1.0$: the low-efficiency stage (left) and the reference stage (right)

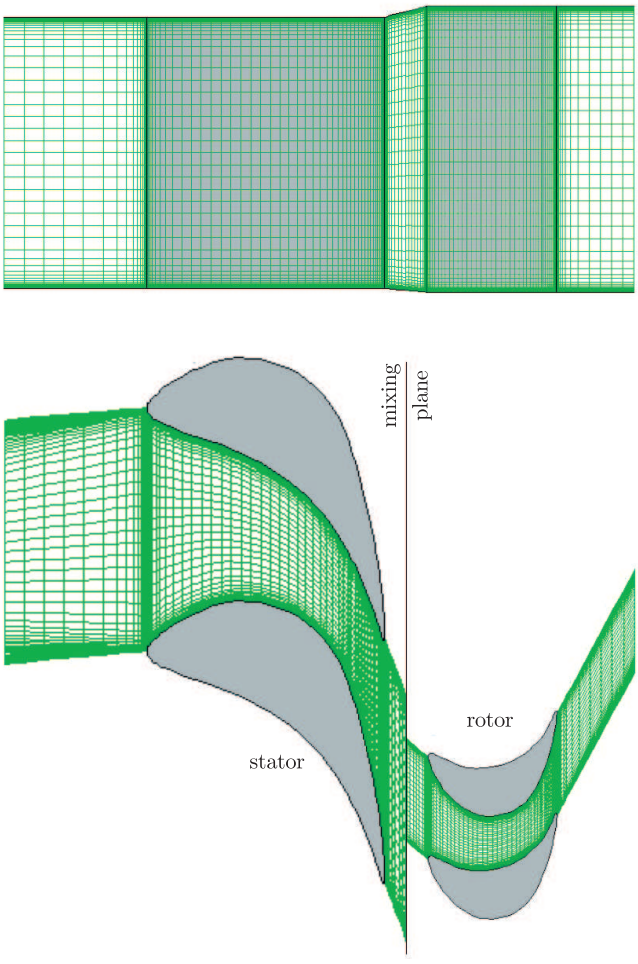

Figure 3. Stage geometry and moderate-resolution grid (third level): section $x0z$ (up) and section $y0z$ (down)

in the entire flow area. For obvious reasons, the final third-level gridline pattern for the selected grid cannot be presented graphically. But in order to present the basic features of the grid, sample gridline distributions in selected $x0y$ and $y0z$ sections are shown in Figure 4 – for the first level of a three-level multigrid structure.

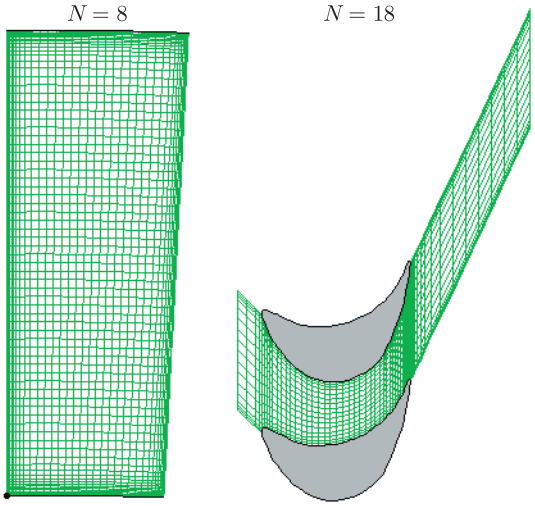

Figure 4. Gridline pattern in fine-resolution grid: rotor passage inlet section $x0y$ (left) and rotor passage midspan section $y0z$ (right); first level of grid resolution

The flow calculations were performed using FlowER, a specialised CFD code for calculating flows through rotating machine stages and stage sections [5]. In this analysis the code solved the set of steady-state RANS equations, complemented by the SST turbulence model. The calculations made use of the three-level multigrid procedure, with 4 000 iterations on the first-level grid and 4 000 on the second-level grid. Basic kinetic and thermodynamic conditions for the flow calculations were taken from a real turbine stage in operation in a Polish power plant. They included:

- total pressure at stage inlet, $p_{0c} = 79.32$ bar;
- total temperature at stage inlet, $T_{0c} = 746.3$ K;
- inlet flow angle in circumferential plane, $\alpha_0 = 0°$;
- inlet flow angle in meridional plane, $\gamma_0 = 0°$;
- static pressure at stage exit, $p_2 = 71.16$ bar.

3. Methodology of investigations

A standard methodology of steady-state flow analyses consists in performing calculations until convergence is reached, and then the obtained results are analysed as time-independent quantities. For the majority of past analyses done using FlowER, the maximum number of iterations after which the flow through the turbine stage could be considered steady was between 14 000 and 16 000, including 8 000 of those done on coarse-level grids. As stated above, however, the investigations were focused on capturing the horseshoe vortex development in the rotor passage in complex flow conditions, with a possible interaction with the separation structures. What is more,

the total force time-history obtained from the calculations performed on the fine-resolution grid revealed remarkable periodical fluctuations, the effect which had not been observed on the moderate-resolution grid. All this was the reason why a decision was made to record instantaneous distributions of flow parameters every 250 iterations, starting from iteration 14 000 when the flow could be considered "periodically stable", *i.e.* more or less free from numerical disturbances. This procedure is similar to that used in unsteady analyses, with a remarkable difference that the length of the time period for the fluctuations to be recorded was not precisely known *a priori*. The calculations were stopped after 24 000 iterations, *i.e.* approximately after two periods of total force fluctuations, roughly assessed from preliminary calculations.

4. Horseshoe vortex development in the rotor passage of the reference stage

The formation and development of horseshoe vortices in the vicinity of blunt bodies has been the object of numerous studies, see [6, 7] for instance. In the majority of cases, the examined blunt body has been symmetrical, rendering it impossible to examine the effect of body curvature and resultant different pressure gradients on the suction and pressure sides. The below presented results have been obtained for a real turbine stage, here referred to as the reference stage in which the formation of regular and stable horseshoe vortices has been observed. These results can be considered representative for a variety of turbine stages with cylindrical rotor blades.

When the turbulent boundary layer forming at a turbine endwall approaches a rotor blade, the adverse pressure gradient generated by the blade deforms it into a so-called horseshoe vortex. The front part of this vortex is situated at a distance upstream of the rotor blade leading edge and the two legs, the remaining parts of the vortex structure extend downstream into the rotor passage. In the central part of the vortex the rotation vector is perpendicular to the main flow, see Figure 5, while the vortex legs inside the rotor passage are nearly parallel to it.

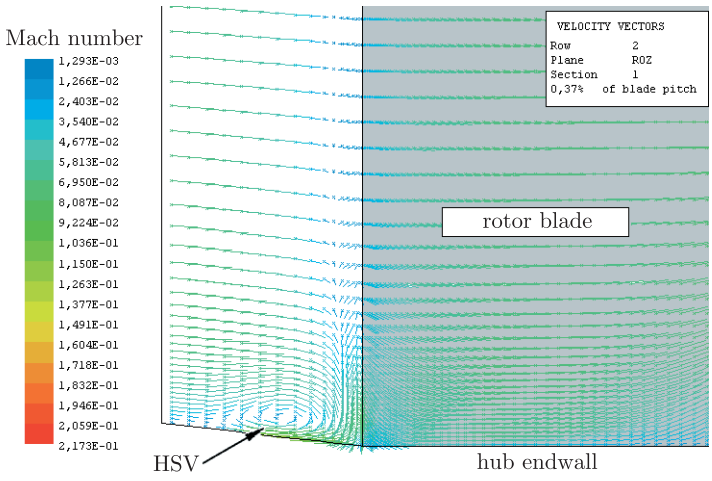

Figure 5. Horseshoe vortex formation at rotor blade leading edge

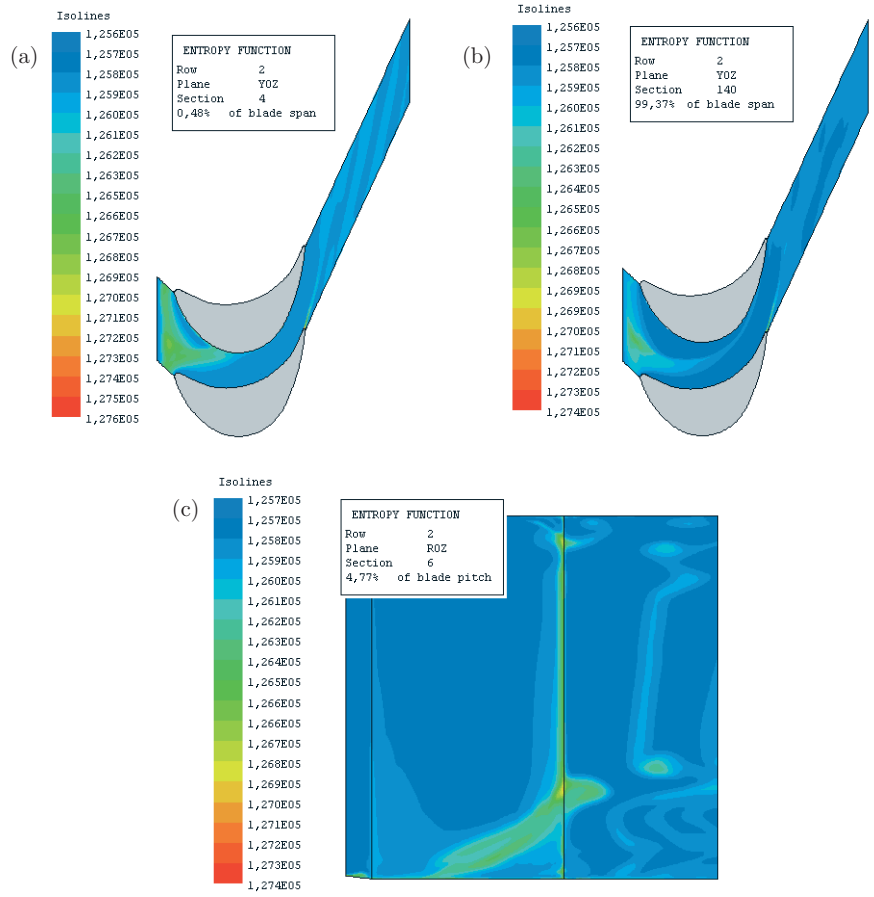

Figure 6. Horseshoe vortex patterns: (a) hub endwall $x/l = 0.48\%$, (b) tip endwall $x/l = 0.48\%$, (c) $x0z$ section $y/t = 4.77\%$ from the rotor blade suction side

Selected patterns of the horseshoe vortices are shown in Figure 6 presenting entropy distributions in the area of horseshoe vortex formation. Figure 6a shows the vortex near the hub endwall. A series of horseshoe vortices situated near rotor blades form a relatively regular front of increased entropy upstream of the blade row. One of the vortex legs, with clockwise circulation, which protrudes from this front is shifted towards the suction side of the rotor passage. After approaching the blade, the vortex moves up, reaching about 20–30 percent of the blade span at the rotor exit, Figure 6c. A qualitatively similar pattern of vortex development can be observed at the tip endwall, but this time the counterclockwise leg, visibly weaker than that of the hub vortex, is situated in the centre of the passage.

A series of entropy distributions in successive $x0y$ sections situated at dimensionless z/c distances, where c is the length of the rotor blade chord projection on the turbine axis, equal to: 0.2, 0.5, 1.0 and 1.2 from the rotor blade leading edge is shown in Figure 7 (left). The horseshoe vortices presented here are regular, even for the most distant section $z/c = 1.2$ showing an interaction of the horseshoe vortices with the rotor wake. The secondary velocity vector distribution in this section shows that

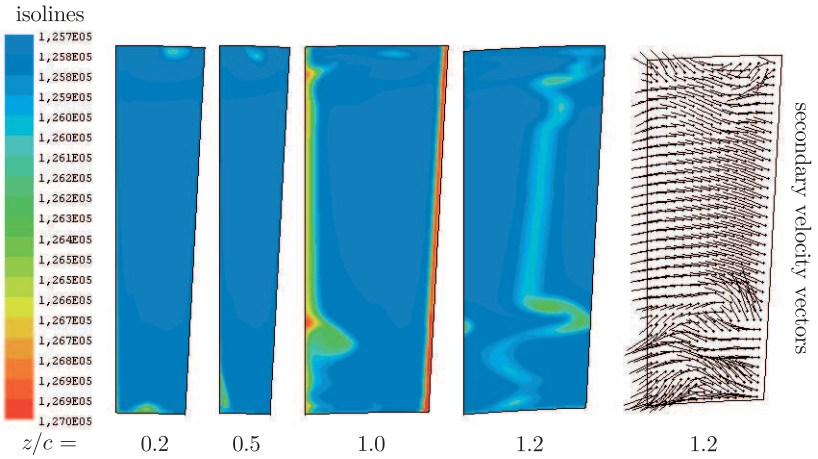

Figure 7. Horseshoe vortex development in the reference stage rotor: left – entropy distributions; right – secondary velocity vector

the flow between the hub and tip vortices is regular, and remarkable flow disturbances are observed only in parts between the horseshoe vortex legs and the corresponding tip or hub walls. The flow pattern presented here was obtained after the final iteration, $n = 24\,000$, but an analysis of all intermediate results (not shown here) recorded after each 250 iterations between iteration 14 000 and 24 000 has revealed no visible changes.

5. Horseshoe vortex interaction with separation structures

In the low-efficiency stage the formation and development of the horseshoe vortices took a more complicated course, see Figures 8–9. Like in the reference stage, the vortices form upstream of the rotor blade leading edge. While inside the rotor passage, the hub vortex's clockwise-rotation leg moves towards the passage suction side, $z/c = 0.1-0.5$, and further up along the blade surface, $z/c = 0.7-1.0$. At the same time the tip vortex's counterclockwise-rotation leg remains approximately in the mid-pitch position. Like in the reference stage, the remaining legs of the two vortices are hardly recognisable. A noticeable difference between this and the reference case is a more complicated structure and different positions of the hub vortex. Here the hub vortex is visibly stronger, and in some diagrams, $z/c = 0.7$ and 0.9 for instance, it reveals a two-core structure. Also the hub vortex position with respect to the hub endwall is much higher than in the reference case. A further interaction of the vortex with the rotor wake leads to the formation of a new structure resembling a vortex pair, *i.e.* two vortices of an opposite rotation sign, see Figure 9 – the secondary velocity vector distribution. Another difference between the flow patterns shown here and in Figure 7 for the reference stage is a much higher complexity of the present flow structure. Unlike the reference flow which could be considered uniform in the major part of the passage section, the secondary flows are observed as high as up to 50–60 percent of the rotor passage height, and the only fragment in section $z/c = 1.2$ which is unaffected by the secondary flows is that located in the upper part of the passage, approximately between 60 and 80 percent of the rotor passage height.

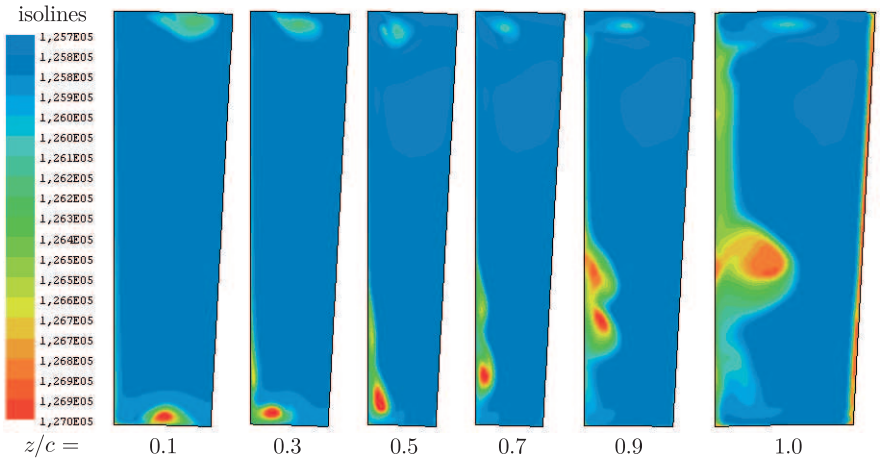

Figure 8. Horseshoe vortex development and interaction with the separation structures inside the rotor passage

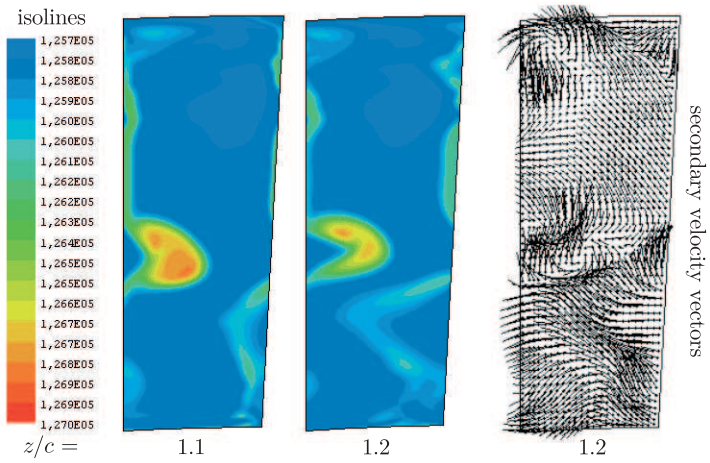

Figure 9. Interaction of the horseshoe vortex with the rotor wake

However, the essential and most remarkable difference between the present case and the reference case is the highly unstable development of the hub horseshoe vortex. This process can be traced in Figure 10, which shows entropy distributions recorded in section $z/c = 0.9$ in consecutive time instants differing by 250 iterations between each other, starting from iteration 14 000 (diagram 1) and ending with iteration 23 750 (diagram 40). As can be observed, the presented collection of diagrams reveals a clear repeatability with the time period approximately covering 20 diagrams. Let us analyse the time-history of the hub horseshoe vortex development starting from diagram 5 in which the hub vortex is in the position similar to that observed in the reference stage. When the time elapses, the vortex grows in intensity and shifts upward along the rotor blade suction side, diagrams 6–19. When it is at about 40–50 percent of the rotor passage height above the hub endwall, the vortex breaks down into two or more smaller structures, diagrams 21 and 22, the lowest of which moves down to the position initially occupied by the hub vortex and the entire process is repeated.

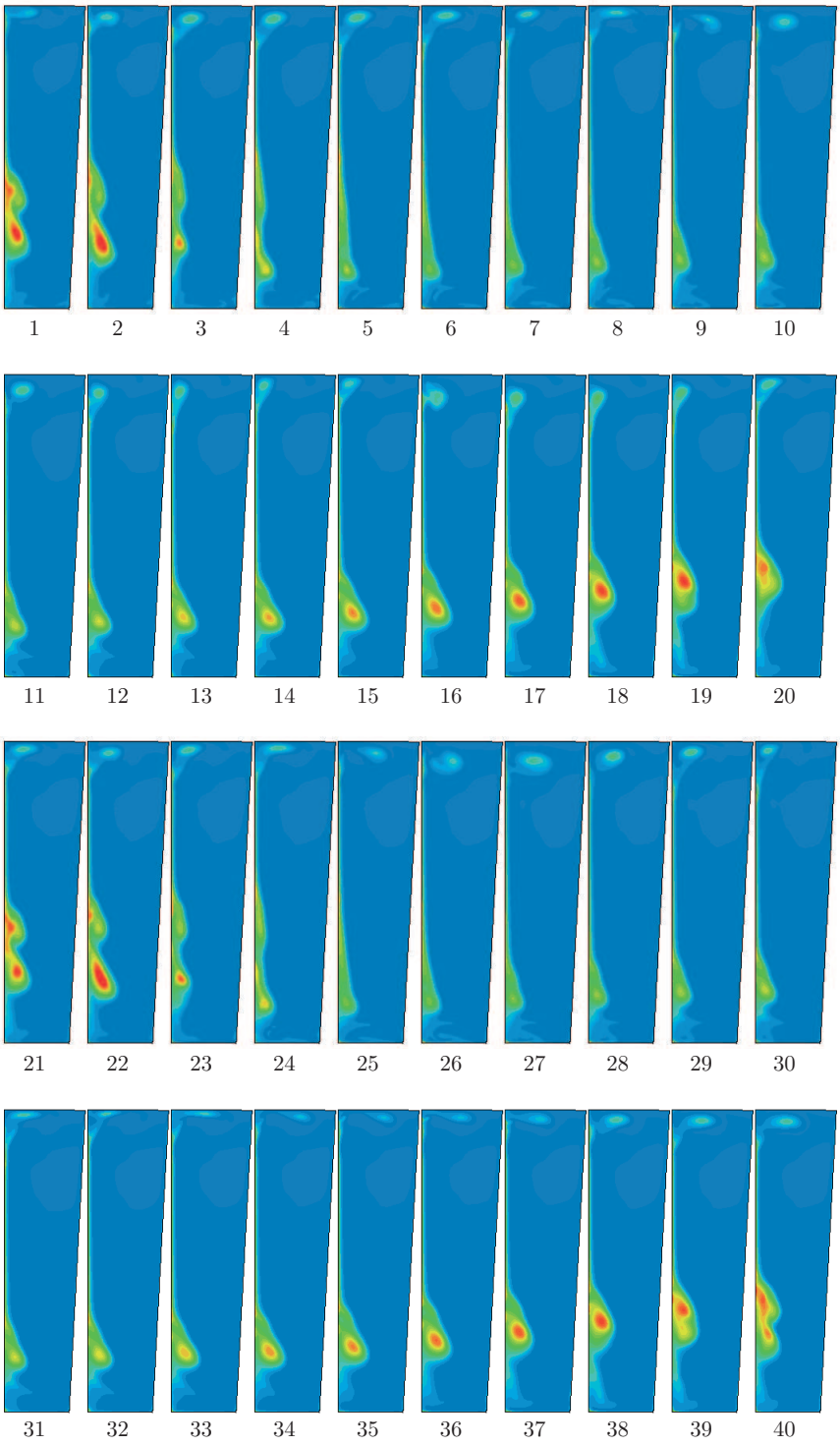

Figure 10. Horseshoe vortex fluctuations: $z/c = 0.9$

It should be stressed at this point that the above presented periodic oscillations of the hub horseshoe vortex are observed in the entire rotor passage area, even in sections that are close to the rotor blade leading edges, $z/c = 0.1$ and 0.3. However, their scale is obviously much more limited.

The physical nature of the reported instability in the horseshoe vortex development is not clear. A factor which most likely provokes it is the presence of the separation zone in the rear part of the rotor passage. This effect was not recorded in the reference stage, in which the hub horseshoe vortex was relatively stable, only revealing minor irregular oscillations around the central position. According to the vortex dynamics theory, when a two-dimensional vortex is placed in the vicinity of a flat plate, its behaviour can be modelled by placing a mirror vortex of an opposite rotation sign on the other side of the plate, thus creating a vortex pair. The speed of the translatory motion of this vortex pair depends on the strength of the vortices and the distance between them. These two-dimensional rules cannot be directly applied to the present three-dimensional situation. However, they are still valid for certain fragments of the hub horseshoe vortex, the final shape of which, seen in Figure 6, is the effect of some sort of an equilibrium between all forces acting on the vortex. When the vortex does not change its strength, its shape and position occupied in the rotor passage remain stable, see the reference case. On the other hand, the vortex's growing strength is a source of an extra unbalanced force which pushes certain parts of the vortex upwards in the examined situation, as can be observed in Figure 10. When the vortex strength exceeds some limit it makes the vortex break down into smaller structures. But questions which are still open here are why and how the hub horseshoe vortex collects energy from the separation flow in the time interval when it increases its strength, and what is the real trigger which makes the vortex break down. Unfortunately, detailed studies of these problems go beyond the scope of this article and are not in line with its present goals.

The tip horseshoe vortex is also more unstable than in the reference case. However, its movements are not as regular as those of the hub vortex, see upper parts of the diagrams in Figure 10. The time of its oscillations is visibly shorter and seems to last from six to eight recordings presented in Figure 10, see diagrams 1–8, 15–20, and 24–30.

6. Conclusions

The aim of the investigations discussed in the article has been to check the ability of the CFD code to study the development and interaction of vortex structures in a turbine rotor passage, and collect possible patterns of behaviour of the horseshoe vortices forming in this area. Based on the results presented in the article the following conclusions can be formulated:

1. CFD calculations performed on grids with resolution of an order of 2 000 000 cells per passage can make an effective basis for studying the formation and development of vortex structures in turbine stage row passages.
2. In turbine stages revealing good performance characteristics, the development of horseshoe vortices in the rotor cascade takes a regular course, and the behaviour of these vortices is stable and regular.

3. When a turbine stage reveals poorer performance characteristics due to the presence of separation zones in the rear parts of the cascade passages, the interaction of the horseshoe vortices with the separation structures formed in this area may take a more unstable and periodic course, and be a source of recordable fluctuations of stage flow parameters.

The above conclusions are of considerable importance and applicability for studying complex unsteady phenomena such as stator/rotor interactions, or stator (rotor) clocking in real turbine stages.

References

[1] Arnone A, Pacciani R and Sestini A 1995 *ASME J. Fluids Engng* **117** 647
[2] Arnone A and Pacciani R 1996 *ASME J. Turbomachinery* **118** 679
[3] Kost F, Hummel F and Tiedemann M 2000 *Proc. ASME TURBO EXPO 2000*, Munich, Germany, Paper 2000-GT-432, 11 p.
[4] Świrydczuk J 2006 *Systems – J. Transdisciplinary Systems Science* **11** 284 (in Polish)
[5] Yershov S V and Rusanov A V 2001 *TASK Quart.* **5** 459
[6] Praisner T J and Smith C R 2006 *ASME J. Turbomachinery* **128** 747
[7] Praisner T J and Smith C R 2006 *ASME J. Turbomachinery* **128** 755